

# Curated Collaborative AI Edge with Network Data Analytics for B5G/6G Radio Access Networks

Sardar Jaffar Ali<sup>1</sup>, Syed M. Raza<sup>2</sup>, Duc-Tai Le<sup>3</sup>, Rajesh Challa<sup>4</sup>, Min Young Chung<sup>3</sup>, Ness Shroff<sup>5</sup>, Hyunseung Choo<sup>3,\*</sup>

<sup>1</sup>Dept. of AI Systems Engineering, Sungkyunkwan University, Suwon, South Korea

<sup>2</sup>James Watt School of Engineering, University of Glasgow, Glasgow, United Kingdom

<sup>3</sup>Dept. of Electrical and Computer Engineering, Sungkyunkwan University, Suwon, South Korea

<sup>4</sup>Core and Automation, Samsung R&D Institute, Bangalore, India

<sup>5</sup>Department of Electrical and Computer Engineering, Ohio State University, Columbus, USA

\*Corresponding author (choo@skku.edu)

**Abstract**—Despite advancements, Radio Access Networks (RAN) still account for over 50% of the total power consumption in 5G networks. Existing RAN split options do not fully harness data potential, presenting an opportunity to reduce operational expenditures. This paper addresses this opportunity through a twofold approach. First, highly accurate network traffic and user predictions are achieved using the proposed Curated Collaborative Learning (CCL) framework, which selectively collaborates with relevant correlated data for traffic forecasting. CCL optimally determines whom, when, and what to collaborate with, significantly outperforming state-of-the-art approaches, including global, federated, personalized federated, and cyclic institutional incremental learnings by 43.9%, 39.1%, 40.8%, and 31.35%, respectively. Second, the Distributed Unit Pooling Scheme (DUPS) is proposed, leveraging deep reinforcement learning and prediction inferences from CCL to reduce the number of active DU servers efficiently. DUPS dynamically redirects traffic from underutilized DU servers to optimize resource use, improving energy efficiency by up to 89% over conventional strategies, translating into substantial monetary benefits for operators. By integrating CCL-driven predictions with DUPS, this paper demonstrates a transformative approach for minimizing energy consumption and operational costs in 5G RANs, significantly enhancing efficiency and cost-effectiveness.

**Index Terms**—Edge architecture, distributed edge learning, collaborative learning, network traffic prediction, DU pooling, sustainable RAN.

## I. INTRODUCTION

**M**ULTI-ACCESS Edge Computing (MEC) is a key enabler of Ultra-Reliable Low Latency Communication (URLLC) services in Beyond 5G (B5G) networks, by placing computing capabilities at the network edge [1]–[5]. In modern Radio Access Networks (RAN), MEC integrates with the network architecture to bring computation closer to users, enabling faster and more efficient processing. To support this, the Open Radio Access Network (ORAN) specification established a split of the traditional Baseband Unit (BBU) into a Central Unit (CU) and Distributed Unit (DU) [6]. The CU, located in Edge Clouds (ECs), manages non-real-time functions such as packet routing, while the DU, positioned at each Base Station (BS) alongside the Radio Unit (RU), manages real-time tasks such as signal processing, ensuring

URLLC services. However, keeping DU servers active at all BS during low-traffic periods leads to unnecessary energy consumption and, consequently, higher operating expenses (OpEx) for operators. This creates an opportunity to reduce OpEx by redirecting traffic from low-traffic DU servers to the nearest available servers, capable of handling the traffic load while maintaining latency requirements. This requires an efficient traffic prediction framework that integrates with the distributed B5G architecture and outperforms existing learning approaches.

A common approach to traffic prediction relies on a centralized Global Learning (GL) that aggregates data from all edge nodes. While straightforward, it suffers from scalability and privacy issues due to high data transmission overhead [3]. Individual Edge Learning (IdEL) mitigates this by training local models at each EC, enabling fast, localized decisions but at the expense of network-wide accuracy. Federated Learning (FL) improves prediction while preserving privacy by collaboratively training a shared model without transferring raw data, as shown in Fig. 1(a). However, FL struggles with non-IID data in B5G/6G networks, resulting in degraded global model performance [4]–[7]. Cyclic Institutional Incremental Learning (CIIL) trains models sequentially across institutions but risks catastrophic forgetting and fails to capture asymmetric traffic patterns [8], [9]. These limitations highlight the need for a novel learning approach tailored to the challenges of B5G distributed architecture and traffic prediction.

This paper proposes Curated Collaborative Learning (CCL), a method designed to optimize traffic prediction and enable DU pooling. CCL builds on the Collaborative Learning (CL) framework proposed in [10], which facilitates the sharing of partial trainable model parameters among selected edge models, eliminating the need for a centralized global model for real-time inferences. However, unlike mobility prediction, where collaboration among distant edges improves performance, traffic patterns across edges tend to be similar, making direct collaboration less effective. Instead, here the edges are further divided into logical clusters based on unique traffic pattern variations, and only clusters with high correlation collaborate. The collaboration framework is structured around

three key questions: whom, when, and what to collaborate.

- “Whom” selects collaborators based on traffic correlation, ensuring that each logical cluster collaborates exclusively with the members of its established collaboration set  $C$ .
- “When” determines the optimal collaboration frequency using validation loss, as both excessive and insufficient collaboration can degrade prediction performance.
- “What” identifies the model parameters to share with members of the collaboration set for maximum performance. In CCL, only the parameters of the initial model layers are shared, while the remaining layers are trained locally, balancing generalization and local adaptation.

CCL has been validated using a real-world cellular traffic dataset from a major operator in Pakistan. It outperforms other methods, including GL, IdEL, FL, Personalized FL (PFL), and CIIL, with accuracy improvements of 28.2%, 32.1%, 39.2%, 33.5%, and 29.7%, respectively. These results demonstrate its effectiveness for traffic prediction and DU pooling.

Leveraging traffic prediction from CCL, a DU Pooling Scheme (DUPS) is proposed to optimize energy consumption in RAN. In DUPS, a deep reinforcement learning (DRL) agent at each BS decides whether to switch a DU server on or off. A centralized critic evaluates the overall reward based on factors such as energy consumption, latency, and penalties for violations. The critic then proportionally distributes the advantages among the agents according to their contributions to the total reward. This adaptive approach dynamically adjusts the number of active DU servers according to the traffic demand at each network edge, significantly reducing energy consumption during low-traffic periods. Additionally, DUPS also includes a routing mechanism to efficiently redirect traffic from deactivated DU servers to the nearest active ones, ensuring smooth resource utilization. Results from the same dataset, benchmarked against conventional strategies, demonstrate that the DUPS effectively reduces the number of active DU servers, consequently reducing energy consumption by up to 89%, and ultimately, reducing OpEx.

The major contributions of the paper are summarized below.

- A proposed AI-driven framework for distributed edge architecture to reduce RAN energy consumption through predicted traffic and resource availability-aware DU pooling, while adhering to latency constraints. Energy consumption has been reduced by up to 89% during low-traffic hours compared to the state-of-the-art.
- A strategic CCL mechanism using multitask DL models in edge clouds ECs, i) exploiting similarity in traffic patterns to determine whom to collaborate with, ii) observing training progress to set when to collaborate, and iii) defining what to collaborate. The novelty improves the prediction performances by an average of 33% compared to other learning approaches.
- A multi-agent DRL framework at each EC that, using the predictions from the CCL, establishes a trade-off between energy consumption, latency, and rejection rate by selecting optimal DU pools.
- A comprehensive performance evaluation using a real-world network traffic dataset from a large city-wide

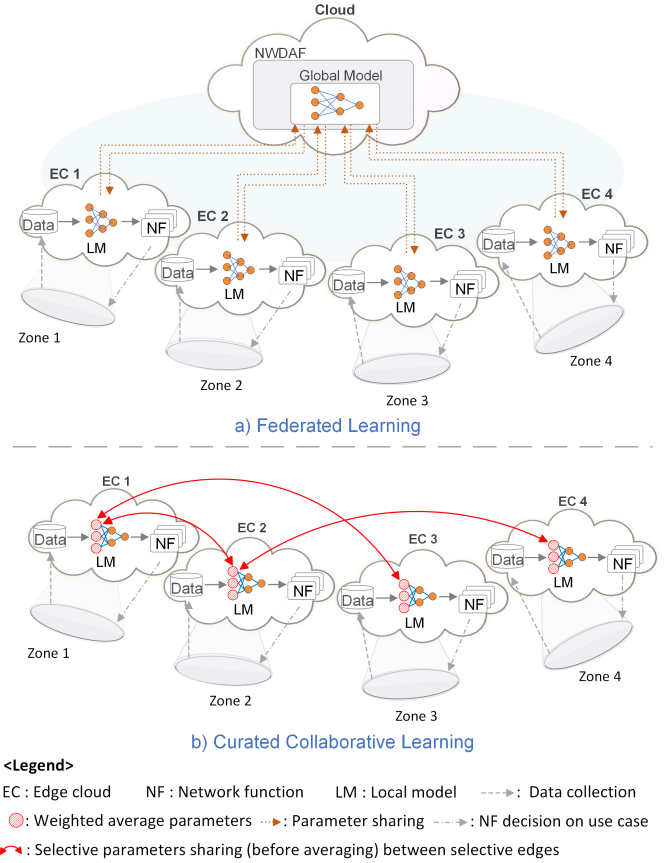


Fig. 1. Conceptual framework comparison of FL and CCL.

mobile network, demonstrating that the proposed CCL and DUPS achieve lower Mean Absolute Error (MAE) and reduced energy consumption, respectively, compared to their respective state-of-the-art counterparts.

The paper is organized as follows: Section 2 provides a brief overview of existing learning frameworks, related studies on traffic prediction, and academic and industry literature on DU pooling. Section 3 details the proposed CCL for traffic forecasting and its integration into the DUPS. Section 4 evaluates the performance of CCL for traffic prediction and DUPS, comparing them with their respective state-of-the-art. Finally, Section 5 concludes the paper.

## II. RELATED STUDIES

This section provides a comprehensive overview of various learning approaches widely proposed for 5G networks, followed by recent state-of-the-art studies targeting traffic forecasting using any of the mentioned learning approaches. Finally, the related work for DU pooling strategies by academia and industry is discussed.

### A. Distributed learning approaches

Machine Learning (ML) traditionally relied on centralized “big data” training, where data was collected and processed in the cloud. Although straightforward, this approach incurs high communication costs and privacy risks. To overcome

these issues, distributed “small data” processing at the edge has gained traction, enabling real-time ML training with minimal data transfer. FL facilitates this by allowing agents to collaboratively train models while keeping data local, preserving privacy, and maintaining accuracy [11], [12]. Multi-agent reinforcement learning builds on FL by enabling distributed decision-making through deep networks [13], but its application in large-scale wireless systems is hampered by significant communication overhead. Personalized Federated Learning (PFL) addresses non-IID data issues by enabling federated multitask learning [14], [15], allowing devices to perform correlated but distinct tasks. Despite these advances, there remains a need for adaptive and efficient distributed learning methods that maximize data utility while ensuring privacy.

To further improve the efficiency of distributed edge environments, the authors of [8] investigated data-private CL methods in the medical science domain, adopting a sequential training approach across institutions rather than parallel training. In this method, each institution trains the model before passing it to the next, continuing until all have completed the process. However, this serial approach can lead to catastrophic forgetting, where the model favors the most recently seen data [9]. An effective alternative involves iterative computation of model weight updates from batches that combine data across multiple non-IID institutional datasets, rather than averaging updates from institution-specific batches [16]. A recent paper proposes a collaborative distributed Network Data Analytics Function (NWDAF) architecture for 5G, enhancing NF data localization, security, and training efficiency while reducing control overhead and improving accuracy through real-time network data testing [17]. However, this architecture includes additional global model training logical functions for each NF, which increases network overhead and cost. In particular, to the best of our knowledge, no prior work has addressed network traffic prediction within the CL architecture.

### B. Traffic forecasting

ML techniques have gained significant attention for network traffic prediction, leveraging models such as ensemble methods and tree-based algorithms. For instance, an ensemble strategy incorporating bagging and a light gradient boosting machine has been proposed to enhance prediction accuracy [18]. Similarly, the sensitivity of ML-based traffic prediction models to dataset variations has been highlighted, emphasizing the impact of data quality on model performance [19]. Furthermore, linear ML models and ensembles have been explored for mobile traffic prediction, demonstrating the need for data preprocessing despite their interpretability and efficiency [20]. However, traditional ML models struggle with complex traffic patterns and datasets, which require more advanced techniques.

To overcome these limitations, researchers have adopted deep learning, particularly time-series models such as Recurrent Neural Networks, Long Short-Term Memory (LSTMs), and Gated Recurrent Units (GRUs), to capture temporal dependencies in network traffic [21], [22]. An enhanced GRU model

has also been introduced for satellite network traffic prediction [23]. However, since traffic data involves spatial correlations, time-series models alone are insufficient. Convolutional approaches, such as graph convolution with LSTM, improve accuracy by capturing spatiotemporal patterns [24]. Likewise, CNN-LSTM and CNN-GRU models have proved effective in environments with multiple access points [25], [26]. These studies demonstrate that while convolutional deep learning methods improve prediction accuracy, optimizing training strategies for real-world data remains essential. Ultimately, accurate traffic forecasting is crucial for operators to optimize DU server allocation and reduce OpEx efficiently.

### C. DU pooling

The disaggregation of traditional BBUs into separate RU, DU, and CU components in ORAN is a fundamental shift in 5G networks, enabling flexible configurations tailored to service requirements [2]. The RU manages radio frequency functions, while the DU, deployed on Commercial Off-The-Shelf (COTS) servers at BS sites, executes real-time Layer 1 and lower Layer 2 functions, ensuring low latency. The CU, responsible for non-real-time higher Layer 2 and Layer 3 functions, centralizes control over multiple DUs. Communication between these components occurs via FrontHaul (FH), MidHaul (MH), and BackHaul (BH) links, facilitating functional splits that enhance centralization, virtualization, and optimized placement decisions [27].

Researchers have investigated DU and CU placement strategies, often neglecting operational costs and functional split constraints. Traffic-aware CU pooling has been proposed to reduce power consumption while keeping DUs at each BS, employing Mixed Integer Linear Programming (MILP) and heuristic algorithms with limited improvements [28], [29]. An optimized routing and packet scheduling framework within an O-DU pool enhances processing efficiency for URLLC and enhanced Mobile Broadband (eMBB) services [30], while reinforcement learning improves DU-CU placement in optical transport networks, outperforming heuristic methods in resource allocation [31]. Samsung highlights that decoupling DU functions from hardware mitigates load imbalances, reducing excess resource allocation [32], whereas Fujitsu advocates dynamic resource scaling based on traffic variations, significantly reducing power consumption in low-traffic periods [33]. These insights align with our proposed system, emphasizing efficient DU pooling, adaptive resource management, and cost-effective RAN deployment.

## III. CURATED COLLABORATIVE LEARNING BASED TRAFFIC FORECASTING AND DRL BASED DU POOLING

This study proposes a CCL framework, incorporating multitask learning to simultaneously predict traffic and user count at BSs. Leveraging these predictions, DRL-based DUPS is proposed to dynamically reduce the number of active DU servers with low or no traffic, significantly lowering OpEx. Furthermore, a method is proposed to redirect the traffic from deactivated DU servers to the nearest active ones with sufficient capacity to handle the traffic load.

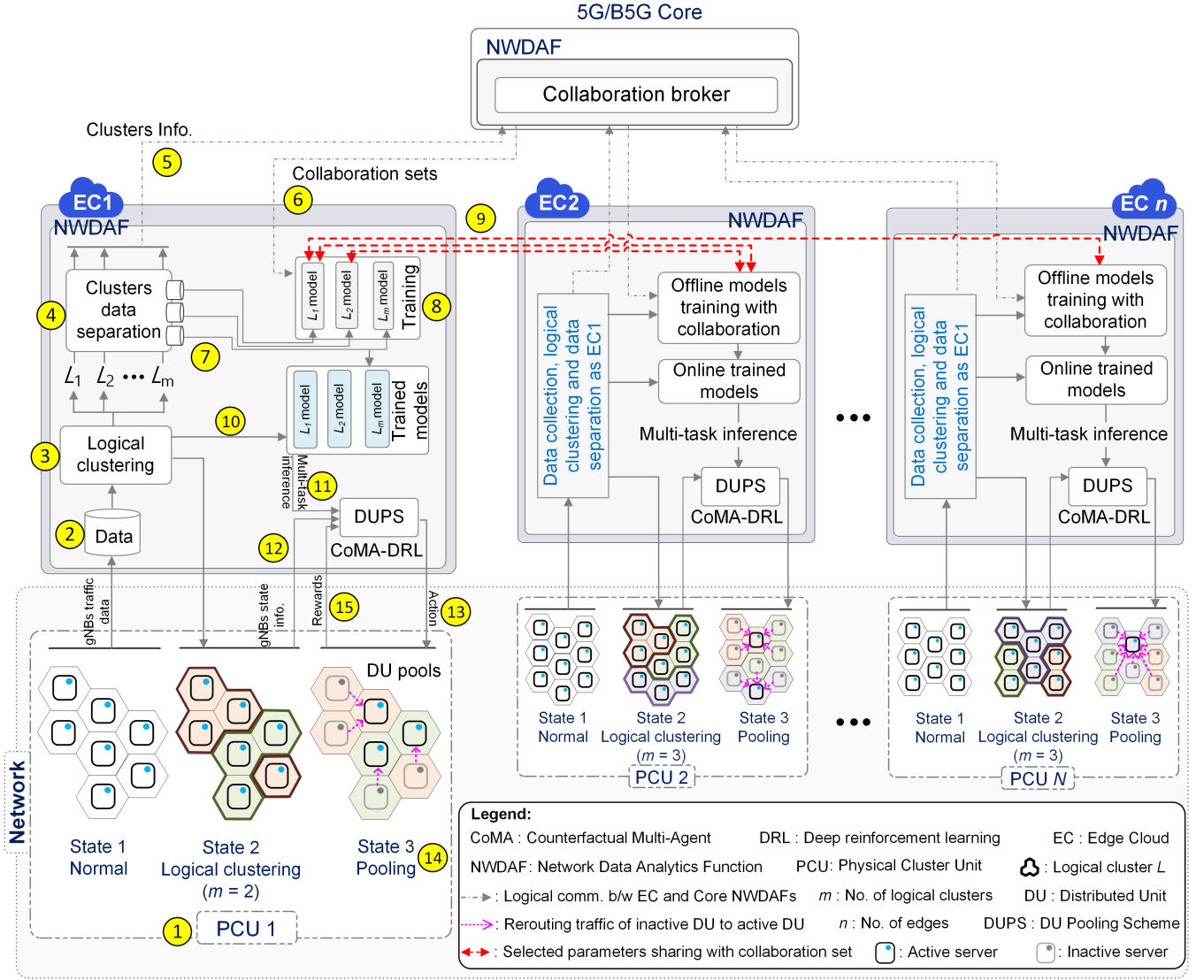


Fig. 2. Curated collaborative learning and DRL-based DU pooling architecture in 5G/B5G.

### A. System architecture

This section provides the overall B5G system architecture, illustrated in Fig. 2, which includes the proposed approaches. The NWDAF collects data and categorizes the BSs into Physical Cluster Units (PCUs) ①. PCUs forward data to their respective ECs for processing ②. Based on traffic correlation using Urbanflow Peak-time Clustering (UPC), NWDAF groups BSs into logical clusters and assigns each cluster a unique logical ID ③. The clustered data is divided into logical clusters ④, and also sent to the 5G core network ⑤ to form collaboration sets  $C$  for collaboration during model training. The core network calculates the correlations among clusters across ECs and sends the collaboration sets back to the ECs ⑥. Each logical cluster then uses its data ⑦ to train models ⑧ and collaborates with other clusters in its  $C$  during the training process ⑨. After offline training, the trained models are used for real-time inference ⑩. The inference ⑪, along with the environment state ⑫, are fed into the

DRL agent for the DUPS, which recommends an action about which DU servers to activate or deactivate ⑬. Traffic from deactivated DUs is rerouted to active ones ⑭. The actions of agents are assessed by monitoring energy consumption with latency and capacity constraints, and the rewards are distributed accordingly ⑮. This approach optimizes network efficiency by turning off underutilized DU servers, pooling traffic to active servers, and adjusting policies for the next cycle.

The first crucial step in the architecture is logical clustering, which groups BSs based on traffic similarities rather than geographic proximity. The rationale for not using PCUs for collaboration is that location-based clusters often overlook relevant traffic patterns of individual BSs. In contrast, logical clusters ensure that prediction models learn from BSs with truly similar trends, improving overall prediction accuracy. Therefore, the UPC method is employed to develop logical clusters at each edge. In the first step, each BS  $b$  is assigned to its peak-traffic cluster  $P_i$ . This is done by identifying



the hour  $i$  when the traffic for a BS is at its maximum, and then grouping all BSs with similar peak hours into the corresponding cluster  $P_i$ . For instance, three BSs  $b_1$ ,  $b_2$ , and  $b_3$  have their peak traffic at 10 AM, and they are assigned to  $P_{10}$ . To create a representative profile for each cluster  $P \in \mathcal{P}$ , where  $\mathcal{P}$  represents the set of all the  $P_i$  in an edge, the average traffic is calculated across all BSs in that  $P$ . For instance, in  $P_{10}$ , if  $b_1$  has traffic values of  $[80, 90, 75, \dots]$ ,  $b_2$  has  $[85, 95, 85, \dots]$ , and  $b_3$  has  $[90, 100, 80, \dots]$ , then the average traffic is  $[85, 95, 80, \dots]$ , forming a representative profile for calculating correlation. The pseudocode for this process is provided in Algorithm S1 in the supplementary materials.

In the next step, the Pearson Correlation Coefficient (PCC) value between all peak-traffic-based clusters  $P_i$  is calculated to quantify the similarity in traffic patterns among all  $P \in \mathcal{P}$ . The PCC measures the linear correlation between two variables, in this case, the traffic patterns of  $P$ . The value of this coefficient ranges from -1 to +1, where -1 indicates a high negative correlation, 0 indicates no correlation, and +1 indicates a high positive correlation between the  $P_i$  and  $P_j$ . The PCC value  $p_{x,y}$  for any two variables  $x$  and  $y$  is calculated as Eq. (1).

$$p_{x,y} = \frac{\sum_{i=1}^h (x_i - \bar{x})(y_i - \bar{y})}{\sqrt{\sum_{i=1}^h (x_i - \bar{x})^2 \sum_{i=1}^h (y_i - \bar{y})^2}} \quad (1)$$

Here,  $\bar{x}$  and  $\bar{y}$  represent the arithmetic mean of the hourly traffic for  $P_i$  and  $P_j$  over  $h$  hours, respectively. Afterward, all  $P$  clusters are consolidated into  $m$  logical clusters within each edge, aiming to maximize the mean PCC within each logical cluster  $L_i$ . For instance, if  $|\mathcal{P}| = 3$ , say  $P_1$ ,  $P_2$ , and  $P_3$ , there are multiple ways to form  $m$  logical clusters. Suppose  $m = 2$ , meaning two logical clusters,  $L_1$  and  $L_2$ . Consider the following configurations where  $L_1 = \{P_1\}$  and  $L_2 = \{P_2, P_3\}$ . In this case, the self-correlation within  $L_1$  is 1, and the pairwise correlation within  $L_2$  is 0.8, yielding an average PCC of 0.9. In another configuration, let  $L_1 = \{P_1, P_2\}$  and  $L_2 = \{P_3\}$ . Here, the pairwise correlation within  $L_1$  is 0.5, and the self-correlation within  $L_2$  is 1, resulting in an average PCC of 0.75, which is lower than the previous configuration. Similarly, the combination  $L_1 = \{P_1, P_3\}$  and  $L_2 = \{P_2\}$  yields a lower PCC value of 0.6. Thus, the final logical clustering will use the configuration that yields the highest average PCC, which in this example is the first combination of  $L_1 = \{P_1\}$  and  $L_2 = \{P_2, P_3\}$ .

### B. Curated Collaborative Learning (CCL)

The proposed collaboration strategy in the architecture is structured into three steps, with details outlined in Algorithms 1 and 2.

1) *Whom to collaborate with? (Setting C)*: The essence of this study lies in its collaborative approach, beginning with the critical task of selecting collaborators and forming a collaboration set  $C$  at the core network, as stated in Algorithm 1. When predicting BS traffic, there is a considerable likelihood that two edges exhibit similar traffic patterns, which does not accurately reflect the actual differences between the traffic of individual BSs. Therefore, it is more effective to collaborate at the level

---

#### Algorithm 1: Construction of collaboration set

---

**Input** : List of logical clusters  $\mathcal{L}$  of every edge; hours  $H = \{0, \dots, 23\}$ ; correlation threshold for logical cluster  $\psi$ .  
**Output**: A collaboration set for each logical cluster.

```

1  $\mathbb{L} = \bigcup_{\mathcal{L}} \mathcal{L}$ 
  // Whom to collaborate with?
2 for each logical cluster  $L_i \in \mathbb{L}$  do
3   for  $h \leftarrow 0$  to  $|H| - 1$  do
4      $L_i.\text{traffic}(h) \leftarrow \frac{\sum_{b \in L_i} b.\text{traffic}(h)}{|L_i|}$ 
  // Calculating pairwise PCC among all  $L_i$ 
5 for  $i \leftarrow 0$  to  $|\mathbb{L}| - 1$  do
6   for  $j \leftarrow 0$  to  $|\mathbb{L}| - 1$  do
7      $r_{i,j} \leftarrow \text{PCC between } L_i \text{ and } L_j \text{ using Eq. (1)}$ 
8 for  $i \leftarrow 0$  to  $|\mathbb{L}| - 1$  do
9    $C_i \leftarrow \emptyset$  // Initialize collaboration set
10  for  $j \leftarrow 0$  to  $|\mathbb{L}| - 1$  do
11    if  $i \neq j$  and  $r_{i,j} \geq \psi$  then
12       $C_i \leftarrow C_i \cup \{L_j\}$ 
13 return  $\{C_i \mid i \in \mathbb{L}\}$  // Return the collaboration set for each logical cluster.
```

---



---

#### Algorithm 2: Collaborating frequency and parameters

---

**Input** : Collaboration set  $C$  for logical cluster  $L_i$ ; collaboration frequency threshold  $\omega$ ; validation loss  $v$ ; maximum epochs  $T$ .  
**Output**: Updated parameters  $W$ .

```

1 while 1 do
2   for each epoch  $i$  do
3      $v \leftarrow \frac{1}{2 \times |\text{batch}|} \sum_{\text{data} \in \text{batch}} (\text{MAE}(\text{pred.traffic}, \text{data.traffic}) + \text{MAE}(\text{pred.users}, \text{data.users}))$ 
4     if  $|\nabla v| \leq \omega$  or  $i > \frac{T}{2}$  then
5       break // Stop current training and wait for collaboration.
  // Collaborating parameters
6 for each logical cluster  $L_i \in C$  do
7    $\alpha_i \leftarrow \frac{|L_i|}{|C|}$ 
8    $W \leftarrow \frac{W + \sum_{L_i \in C} \alpha_i \times W_i}{|C| + 1}$ 
9 return  $W$  // Return the updated parameters.
```

---

of logical clusters rather than at the level of entire ECs. The core network computes the pairwise PCC among all  $L \in \mathcal{L}$ , as in lines 1-7. For each logical cluster  $L_i$ , if the value of  $r_{i,j}$  with any  $L_j \in \mathcal{L}$  exceeds a given threshold  $\psi$ , then  $L_j$  is added to the collaboration set  $C_i$  for  $L_i$ , as in lines 8-12. This selective collaboration ensures that the model learns exclusively from correlated models of logical clusters across all edges. Such selective refinement enhances the resilience and adaptability of the model by accommodating out-of-distribution patterns found in any edges from  $C$  but not present in the source model. It is worth noting that this framework is equally applicable to the level of EC collaboration in other prediction tasks when there is a dissimilarity between task patterns of the edges [10].

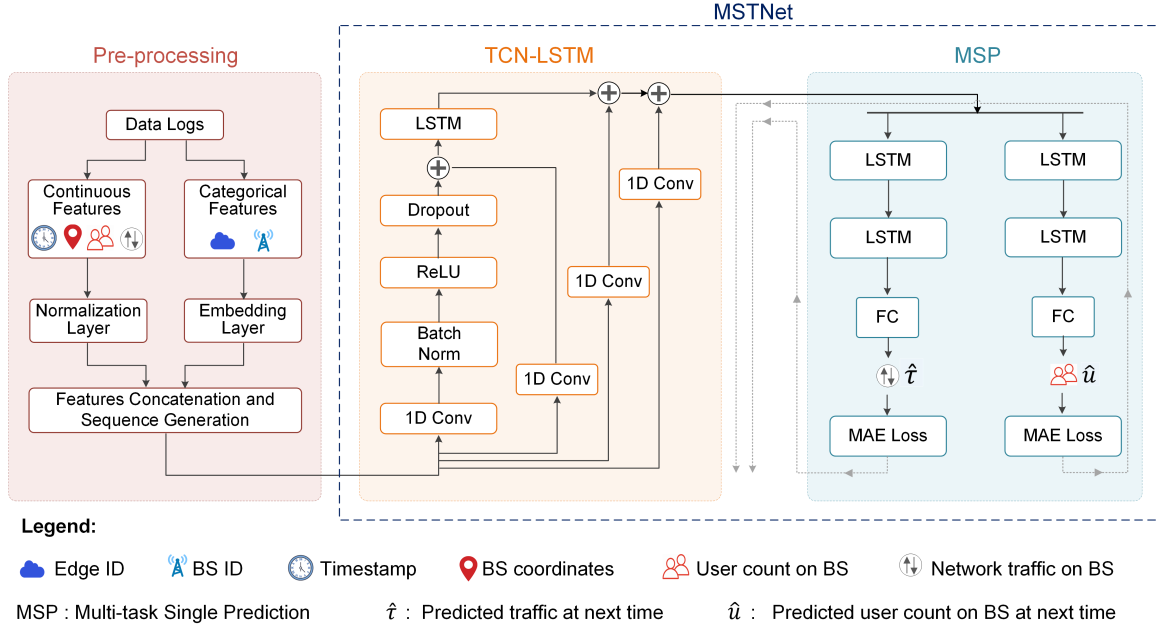


Fig. 3. Multitask Single-step Temporal Network (MSTNet) model for predicting BS next traffic  $\hat{t}$  and user count  $\hat{u}$ .

2) *When to collaborate?* (Setting  $\omega$ ): Sharing parameters before the models have learned meaningful patterns leads to unnecessary overhead and computational inefficiencies. Therefore, determining the right collaboration frequency threshold  $\omega$  is crucial. It is proposed that each collaborating model shares trainable parameters only after learning certain patterns. This could be monitored through  $\nabla v_i$ , the rate of change in the validation loss of the individual logical cluster model  $L_i$  while they train on their data (lines 1-7 of Algorithm 3). For instance, if  $\nabla v_i$  fell below a given threshold  $\omega$ , the model is deemed ready to share its trainable parameters. This approach reduces overhead while maintaining a satisfactory performance.

3) *What to collaborate?*: During offline training, each model trains on its local dataset while selectively sharing the parameters of the initial layers of the logical cluster with collaborators. Extensive evaluations, including ablation studies in [10], demonstrated that collaborating on the initial layers significantly improved generalization. This is because the initial layers are less affected by backpropagation and thus better suited for collaboration. After receiving parameters from collaborators, the source NWDAF model takes a weighted average of the shared parameters and updates the corresponding layers (Algorithm 3, lines 8-10). This approach allows the initial layers to learn from broader patterns across clusters, while the deeper layers continue to learn from local data. It is important to note that the parameters are shared before averaging, ensuring that collaborators receive only the direct contribution from the source model, which helps mitigate the influence of models outside their collaboration set and leads to more effective learning.

While resembling split learning, the key difference lies in the active involvement of all logical clusters in parameter sharing in split learning, where the local model of the logical cluster  $L_x$ , for instance, receives contributions from

all models, potentially compromising its ability to capture local data nuances and performance. On the other hand, our approach shares parameters intelligently between selected clusters within the ECs, which helps them to learn better collectively. This tailored approach improves how accurately BS traffic can be predicted, which can help develop efficient resource allocation strategies.

### C. Multitask Single-step Temporal Network (MSTNet) for CCL

MSTNet, illustrated in Fig. 3, is designed for simultaneous traffic and user count prediction at BSs that encompasses three key components: TCN-LSTM, Residual Connections (RC), and Multitask Single-step Prediction (MSP). TCN-LSTM extracts complex temporal patterns from mobile radio and location data, while RC ensures the retention of long-term dependencies. MSP, structured with two branches, enables joint learning of BS traffic  $\hat{t}$  and user count  $\hat{u}$ , enhancing predictive performance by leveraging their interdependencies.

TCN layer employs 1D dilated causal convolutions to efficiently capture short-term dependencies without increasing model complexity. Batch normalization stabilizes training, while Rectified Linear Unit (ReLU) activation enhances non-linearity, improving pattern extraction. To prevent overfitting, a 20% dropout rate is applied before the LSTM layer, which captures long-range dependencies. Unlike traditional activations that suffer from gradient saturation, ReLU ensures stable backpropagation, making the model robust in learning both short- and long-term correlations. RC further enhances MSTNet feature extraction by linking intermediate and final outputs within TCN-LSTM blocks. These connections allow high-dimensional features to be processed early while refining lower-dimensional representations later, preventing information loss and gradient vanishing. This structured information

flow improves the ability of the model to capture complex patterns.

The MSP block finalizes the architecture with two LSTM-based branches, each followed by Fully Connected (FC) layers for traffic and user count prediction. The traffic branch consists of LSTM layers with 256 and 32 units, followed by a hidden layer with 16 nodes and a single output node. The user count branch follows a similar structure but includes a hidden layer with 8 nodes. Both branches optimize MAE loss functions, given by Eq. (2), ensuring precise predictions. Sequential training integrates the losses from both branches, refining the TCN-LSTM block for optimal performance across both tasks.

$$\ell_{\omega} = \frac{1}{N} \sum_{i=1}^N |\omega_{q+1} - \hat{\omega}_{q+1}| \quad (2)$$

Here,  $\omega_{q+1}$  represents the ground truth, while  $\hat{\omega}_{q+1}$  is the prediction for the next hour ( $q+1$ ).  $\omega$  is either  $\tau$  or  $u$  to predict BS traffic or user count, respectively.

#### D. DRL for DU pooling

Leveraging the most accurate traffic prediction, the proposed DUPS employs a Multi-Agent Deep Reinforcement Learning (MADRL) framework to optimize energy efficiency and minimize service delay in RANs. MADRL is particularly well-suited for DUPS due to its ability to handle multiple agents (DUs) in a decentralized manner, enabling dynamic resource management and adaptability to fluctuating traffic conditions. The problem is formulated as a Partially Observable Markov Game (POMG), where each DU agent interacts with a partially observable environment to make decisions based on local observations and shared information.

1) *Problem formulation*: The POMG is defined by the tuple  $(\mathcal{N}, \mathcal{S}, \mathcal{A}, \mathcal{O}, \mathcal{T}, \mathcal{R}, \gamma)$ . Here,  $\mathcal{N} = \{1, 2, \dots, n\}$  represents the set of agents, corresponding to the number of BSs. The finite state space is denoted by  $\mathcal{S}$ , while the joint action space for all agents is given by  $\mathcal{A} = \prod_{i=1}^n \mathcal{A}^i$ . The joint observation space is defined as  $\mathcal{O} = \{o_1 \times o_2 \times \dots \times o_n\}$ , and the state transition probability is represented by  $\mathcal{T} : \mathcal{O} \times \mathcal{A} \rightarrow \mathbb{R}$ . The reward function  $\mathcal{R} : \mathcal{O} \times \mathcal{A} \rightarrow \mathbb{R}$  provides feedback to the agents, and  $\gamma$  denotes the discount factor for future rewards.

2) *Key components*: The environment consists of a RAN where each BS is managed by a DU controlled by an actor agent. These agents collaboratively address the DU pooling problem by dynamically switching DUs on or off to balance energy efficiency and service performance. At time  $t$ , the state  $s_t = [t, DU_s, \hat{\tau}, \hat{u}]$  includes the current time  $t$ , the DU power state ( $DU_s$ ), the predicted traffic load ( $\hat{\tau}$ ), and the predicted user count ( $\hat{u}$ ) on the BS from MSTNet. Each agent selects an action  $a_t \in \{0, 1\}$ , where  $a_t = 0$  turns the DU off and  $a_t = 1$  turns it on. This action influences both the next state and the reward received. The reward function  $r_t$ , given by Eq. 3, is designed to balance energy efficiency, service delay, and penalties.

$$r_t = \alpha E_t - (1 - \alpha) D_t + \beta P_t \quad (3)$$

Here  $E_t$  represents energy consumption, which is 70% at no load, and scales linearly to 100% at full load.  $D_t$  denotes

#### Algorithm 3: COMA-based DU pooling

---

**Input** : Network insights including timesteps  $t$ ; BS IDs; predicted traffic  $\hat{\tau}$ ; predicted user count  $\hat{u}$ ;  $n$  BSs, each with one active DU server; maximum steps per episode  $T$ ; number of episodes  $e$ ; buffer memory  $M_B$  with capacity  $B$ .

**Output**: Trained policy network  $\pi_{\theta}$ .

---

```

1 Initialize  $n$  DUs for  $n$  BSs, critic network  $\theta_{\text{critic}}^1$ , target critic
  network  $\hat{\theta}_{\text{critic}}^1$ , actor network  $\theta_{\text{actor}}^1$ , and  $M_B$ .
  //  $\lambda$ : Bias-variance tradeoff parameter in
  // Q-value estimation.
  //  $\alpha$ : Learning rate for updating network
  // parameters.
  //  $\gamma$ : Discount factor for future rewards.
2 for each episode  $i \leftarrow 1$  to  $e$  do
  // Step 1: Trajectory collection
3   for each timestep  $t \leftarrow 1$  to  $T$  do
4     Each actor with  $\theta_{\text{actor}}$  selects DU status action
       $a_t^z \in \{0, 1\}$  for DU  $z$ , based on state  $S_t$ .
5     if  $a_t^z = 0$  then
6       | Execute traffic redirection via Algorithm 5.
7     Compute reward  $r_t$  using Eq. (3).
8      $M_B \leftarrow M_B \cup \{t, S_t, A_t, r_t\}$ .
  // Step 2: Critic network update
9   for each timestep  $t \leftarrow 1$  to  $T$  do
10    Unroll states, actions, and rewards from  $M_B$ .
11    Compute target Q-value  $y_t^{(\lambda)}$ :
12     $y_t^{(\lambda)} = (1 - \lambda) \sum_{n=1}^{\infty} \lambda^{n-1} G_t^{(n)}$ , where  $G_t^{(n)} =$ 
       $r_{t+1} + \gamma r_{t+2} + \dots + \gamma^{n-1} r_{t+n} + \gamma^n V(S_{t+n})$ .
      //  $G_t^{(n)}$ :  $n$ -step return with  $V(S_{t+n})$ 
      as the value function from the
      critic network.
  // Step 3: Target critic
  // synchronization
13  for each timestep  $t \leftarrow T$  to 1 do
14    Compute gradient for critic network update:
15     $\Delta \theta_{\text{critic}} = \nabla_{\theta_{\text{critic}}} (y_t^{(\lambda)} - Q(S_t, A_t))^2$ .
16    Update critic network parameters:
17     $\theta_{\text{critic}}^{i+1} = \theta_{\text{critic}}^i + \alpha \Delta \theta_{\text{critic}}$ .
18    Sync target critic network every  $B$  steps:
19     $\hat{\theta}_{\text{critic}}^1 \leftarrow \theta_{\text{critic}}^1$ .
  // Step 4: Actor network update
20  for each timestep  $t \leftarrow T$  to 1 do
21    Compute advantage function  $Z_t^j(S_t, A_t)$  for each
      agent  $j$  using Eq. (4).
22    Update actor network gradient:
23     $\Delta \theta_{\text{actor}}^j = \alpha \nabla_{\theta_{\text{actor}}^j} \log \pi_{\theta_{\text{actor}}^j}(S_t^j, a_t^j) Z_t^j(S_t, A_t)$ .
24    Update actor network parameters:
25     $\theta_{\text{actor}}^{i+1} = \theta_{\text{actor}}^i + \alpha \Delta \theta_{\text{actor}}^j$ .
26 return  $\pi_{\theta}$  // Return the trained policy.
```

---

FH latency, which increases when traffic is redirected to another DU.  $P_t$  represents the penalty for service degradation. The weights  $\alpha$  and  $\beta$  control the trade-off between energy consumption, latency, and constraint violations, allowing the model to balance energy efficiency with service performance.

3) *COMA-based training*: The Counterfactual Multi-Agent (COMA) algorithm is employed to train the agents. COMA utilizes a centralized critic and distributed actors, enabling efficient policy learning through centralized training and de-

centralized execution. The centralized critic computes the Q-values,  $Q(S_t, A_t)$ , for joint state-action pairs and evaluates the advantage function  $Z_t^j(S_t, A_t)$  for each agent  $j$ . The advantage function is defined by Eq. (4) and it quantifies the contribution of each agent's action to the global reward, enabling the actor network to learn optimal policies.

$$Z_t^j(S_t, A_t) = Q(S_t, A_t) - \sum_{a_t^j} \pi^j(a_t^j | S_t^j) \cdot Q(S_t, (A_t^{(-j)}, a_t^j)). \quad (4)$$

4) *Training process*: The training process consists of four main steps, as illustrated in Algorithm 3. First, during trajectory collection, actors select actions  $a_t^i \in \{0, 1\}$  based on the current state  $S_t$ . If  $a_t^i = 0$ , traffic is redirected to the nearest active DU using Algorithm 4. The system transitions to the next state, and the reward  $r_t$  is computed using Eq. (3). Experiences (states, actions, rewards) are stored in a buffer  $M_B$  for subsequent optimization. Second, the critic network is updated by computing target Q-values  $y_t^{(\lambda)}$  using the  $\lambda$ -return method:

$$y_t^{(\lambda)} = (1 - \lambda) \sum_{n=1}^{\infty} \lambda^{n-1} G_t^{(n)}, \quad (5)$$

where  $G_t^{(n)}$  is the  $n$ -step return. The critic is updated by minimizing the loss  $(y_t^{(\lambda)} - Q(S_t, A_t))^2$ .

Third, the actor network is updated using policy gradients and the advantage function  $Z_t^j(S_t, A_t)$ . The gradient is accumulated over timesteps and applied to optimize the actor network. Finally, the target critic network is periodically synchronized with the main critic network to ensure training stability.

5) *Network architecture*: The actor network utilizes the LSTM model to capture temporal dependencies in the state sequence, while the critic network is structured as a feed-forward network with ReLU activation layers and FC layers. Both networks are trained in batch mode with a batch size of 100. The actor network has a learning rate of 0.001, whereas the critic network has a learning rate of 0.005. To enhance training stability, a target critic network is periodically updated.

6) *Traffic redirection*: Algorithm 4 handles traffic redirection by rerouting traffic from inactive DUs to the nearest active DU with sufficient capacity. For each inactive DU  $b$ , the algorithm identifies the nearest active DU  $\hat{b}$  and checks if  $\hat{b}$  can accommodate the combined traffic load ( $b_j.\hat{\tau} + b_i.\hat{\tau} \leq b_j.\text{capacity}$ ). If this condition is met, the traffic from  $b$  is routed to  $\hat{b}$ , and  $\hat{b}$ 's traffic load is updated accordingly.

#### IV. PERFORMANCE EVALUATION

This section evaluates the performance of the two key components of this work. First, for traffic prediction, CCL is compared with several schemes, including GL, IdEL, FL, PFL, and CIIL. Additionally, detailed ablation studies, which explore different variations of CCL along with the computational comparison of CCL with GL, IdEL, and FL in terms of training time, communication overhead, memory usage, and validation loss convergence are provided in the supplementary materials. Leveraging the predicted traffic and user count from the CCL,

#### Algorithm 4: DU pool traffic redirection

**Input** : List of all BS  $\mathbb{B}$ , predicted traffics  $\hat{\tau}$  at each DU server  $b \in \mathbb{B}$ .

**Output**: Routed traffic between DU servers.

```

1 for each base station  $b \in \mathbb{B}$  do
2   if  $b.DU = OFF$  then
3     while 1 do
4        $b' \leftarrow \text{getNextNearestNeighbor}(b)$ ;
5       if  $b'.DU = ON$  then
6         if  $(b'.\text{traffic} + b.\text{traffic}) < b'.\text{capacity}$  then
7           // Route traffic from  $b$  to  $b'$ 
8            $b'.\text{traffic} \leftarrow b'.\text{traffic} + b.\text{traffic}$ ;
9           break;
10 return Updated traffic distribution among DU servers.
```

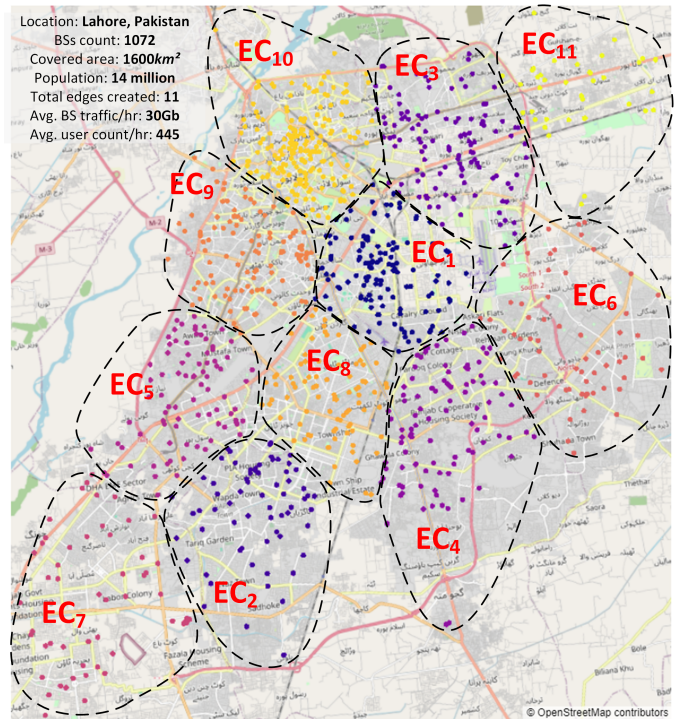


Fig. 4. BSs assignment to 11 Edge Clouds ECs.

DRL-based DUPS is compared with the conventional DU pooling method and MILP scheme for ECs with contrasting traffic conditions. This comparative analysis highlights the improvements by DUPS to improve network sustainability by improving energy efficiency and reducing OpEx. Lastly, the optimal coefficient parameter values used for each EC are determined through experiments detailed in the ablation studies available in the supplementary materials.

#### A. Dataset and Experimental Setup

The CCL and DUPS frameworks are evaluated using a proprietary mobile network traffic dataset from a 4G LTE operator in Lahore, Pakistan. The dataset spans 1072 BSs across 1,600  $km^2$ , with hourly traffic logs collected over



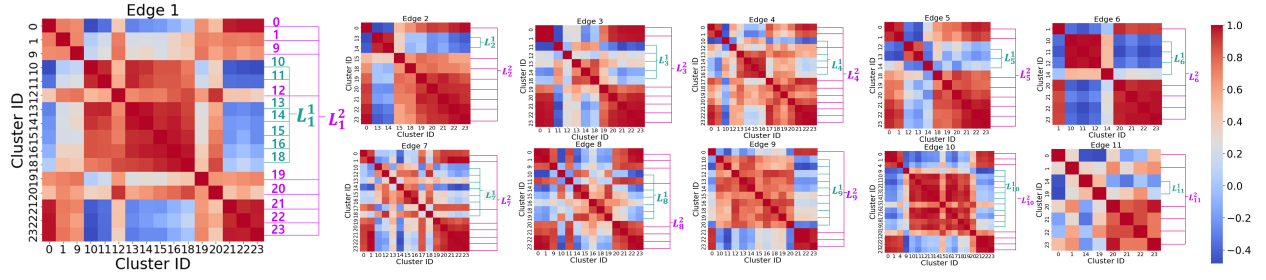


Fig. 5. Urbanflow Peak Clustering (UPC) for 11 edges, where each edge is divided into peak clusters  $P$  based on peak time patterns on the x and y-axis. These clusters are consolidated into  $m = 2$  logical clusters, represented in green ( $L_1$ ) and pink ( $L_2$ ). Each  $L_j^i$  denotes a logical cluster where  $i \in \{1, \dots, 11\}$  represents the edge ID, and  $j \in \{1, 2\}$  is the logical cluster ID.

seven days. Based on insights from prior studies [34], [35], incorporating multivariate features effectively captures diverse traffic variations, ensuring a comprehensive representation of network dynamics over the collected seven-day period. Each record includes the BS ID, sector ID, location, traffic volume, and user count. Missing sector data is corrected via intra-BS averaging, while missing traffic or user values are interpolated using adjacent timestamps. To adapt the LTE dataset for 5G analysis, it is scaled using Eq. (6), considering a 5G BS capacity of 4Gbps [36], [37].

$$DU_i = \frac{4Gbps}{\max\{UserTraffic_{DU_i}\}} \forall DU \in \text{Dataset} \quad (6)$$

Moreover, this cellular network does not employ any ECs in which logical clustering can be done. Thus, the  $k$ -means clustering algorithm is utilized first, aiming to allocate  $n$  BSs to  $k$  ECs. This process is thoroughly explained in the supplementary material and resulted in  $k = 11$  ECs, encompassing 1072 BSs distributed across the city, as shown in Fig. 4.

The primary task is to predict BS traffic. However, these 11 ECs cannot be directly considered for collaboration due to their nearly identical traffic patterns, making such collaboration ineffective. A more effective approach is to further subdivide the ECs into logical clusters  $L$  based on their traffic patterns. Therefore, each edge is further divided into logical clusters according to peak traffic times using UPC. As depicted in Fig. 5, this process produces several peak clusters  $P$  for each of the 11 ECs. For instance,  $EC_1$  has 16 clusters while  $EC_{11}$  has 8. Thus, managing too many clusters within a single edge is impractical and increases computational complexity. Therefore, PCC is applied to merge correlated  $P \in \mathcal{P}$  into **two** logical clusters such that the averaged pairwise PCC is maximum, as explained earlier in the consolidation step of Algorithm S1. The pink and green lines in Fig. 5 illustrate the consolidation of multiple  $P$  into a simplified set of  $m = 2$  logical clusters. For instance, a logical cluster  $L_j^i$  represents  $EC_i$  and its logical ID  $j$  where  $i \in \{1, 2, \dots, 11\}$ , and  $j \in \{1, 2\}$ , given  $m = 2$ .

After forming 22 logical clusters, the average traffic of each cluster is transmitted to the core network, where the correlation matrix between all these logical clusters is calculated, as illustrated in the heatmap Fig. 6. It is evident that a variety of correlations exist among the logical clusters. As discussed

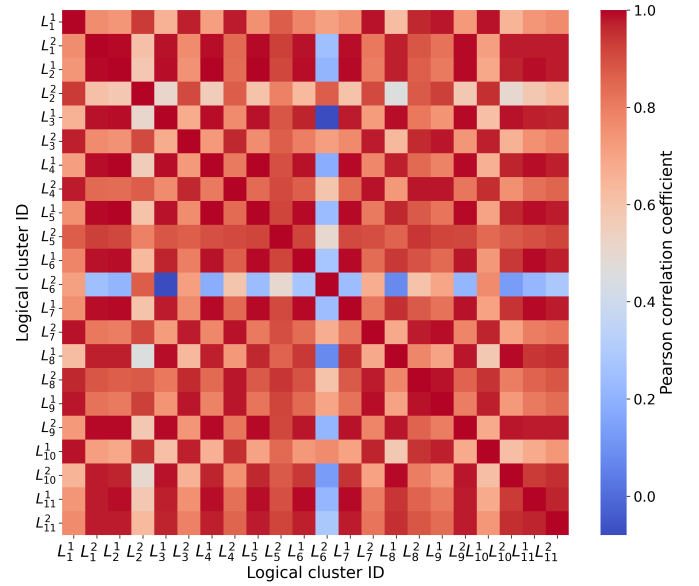


Fig. 6. Correlation between traffic patterns of all  $L \in \mathbb{L}$  from previous Fig. 5.

in Section 3, it is advantageous for each logical cluster to collaborate only with those that exhibit a high correlation. For example,  $L_1^1$  exhibits a higher correlation with twelve other logical clusters, whereas  $L_6^2$  has only  $L_2^2$  in its collaboration set. The core network sends the collaboration sets to the respective logical clusters at their ECs. The correlation threshold value for collaboration is set as 0.95 to ensure that the core network forms the collaboration set of each cluster only with those clusters that have the potential to improve the prediction accuracy of the source cluster.

To this end, all logical clusters have been established, and collaboration sets have been received from the core network. Each  $L$  now receives data from its respective BSs and forms a six-tuple  $\langle \text{time}, \text{edge\_ID}, \text{BS\_ID}, \text{coordinate}, \text{number of users}, \text{traffic} \rangle$ . Sequences of length  $q$  are generated for each BS over time, represented as  $\langle s_1, s_2, \dots, s_q \rangle$ . These sequences are divided into several overlapping input sequences of length  $q$ . For instance, the first input sequence of length  $q = 4$  for any  $BS_i$  is  $\langle s_1, s_2, s_3, s_4 \rangle$ , followed by another sequence  $\langle s_2, s_3, s_4, s_5 \rangle$ , and so on. This approach allows the model to understand the continuous nature of traffic and learn time-

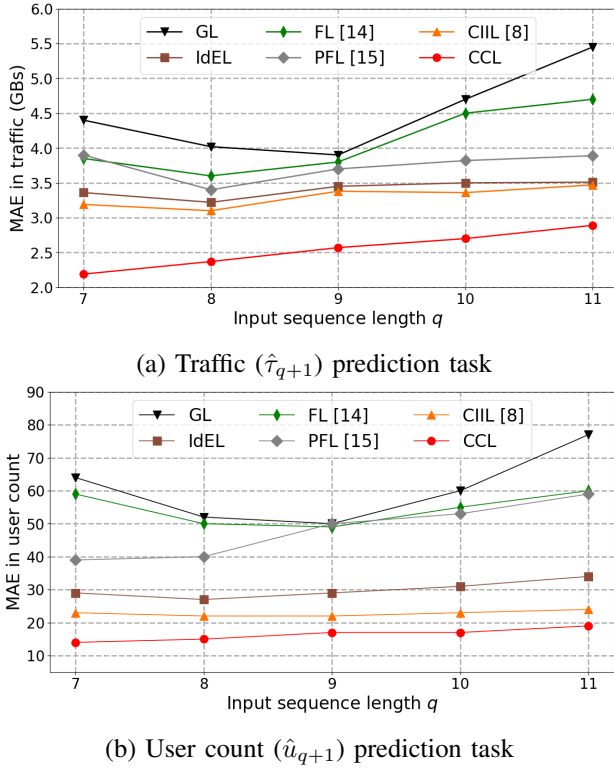


Fig. 7. MAE comparison of CCL with state-of-the-art, averaged across all logical clusters.

series dependencies among the sequences to predict traffic and user counts at  $q + 1$ . The generated sequences are randomly shuffled and split into 70%, 15%, and 15% for training, validation, and testing, respectively.

The traffic and user count predictions are evaluated using MAE, measuring the average absolute error across logical clusters. Training is configured with 1,000 epochs, a batch size of 32, a 0.005 learning rate, and a 0.2 dropout rate to mitigate overfitting. Data is sampled at 60-minute intervals, and the dilated factor, expressed as  $2^i$ , expands the model's receptive field.

## B. Experimental Results

1) *CCL for predicting traffic  $\hat{\tau}$  and user count  $\hat{u}$* : Fig. 7(a) compares CCL with state-of-the-art learning strategies in terms of MAE for predicting  $\tau_{q+1}$  across varying  $q$ . The global model, which employs a single model for all BSs, achieves its lowest MAE of 3.9 GBs at  $q = 9$ , corresponding to a 13% error relative to the dataset's average BS traffic of 30 GBs per hour, as referenced in Fig. 4. IdEL, where each logical cluster trains independently, achieves its lowest MAE of 3.22 GBs at  $q = 8$ , reducing the error to 10.7% by avoiding interference from contrasting traffic patterns. FL achieves its lowest MAE of 3.6 GBs at  $q = 8$ , corresponding to a 12% error, though it still suffers from uncorrelated BSs influencing the learning process. PFL improves upon FL with a minimum MAE of 3.7 GBs at  $q = 9$ , benefiting from local fine-tuning after global updates. CIIL, which sequentially trains across logical clusters, reaches its lowest MAE of 3.19 GBs at  $q = 7$ , reducing the

error to 10.6%. CCL outperforms all approaches, achieving the lowest MAE of 2.19 GBs at  $q = 7$ , corresponding to a 7.3% error.

The task of user count prediction  $\hat{u}$  in Fig. 7(b) follows trends similar to traffic prediction. The GL approach achieves its lowest MAE of 50 at  $q = 9$ , corresponding to an 11.2% error relative to the dataset's average user count of 445 per BS (see Fig. 4). IdEL improves upon this, achieving its lowest MAE of 27 at  $q = 8$ , reducing the error to 6.1% by learning localized patterns. FL reaches its minimum MAE of 49 at  $q = 9$ , corresponding to an 11% error, while PFL further refines FL's performance, achieving an MAE of 39 at  $q = 7$ , yielding an 8.8% error. CIIL significantly enhances prediction accuracy, reaching its lowest MAE of 22 at  $q = 8$ , representing a 4.9% error. CCL outperforms all approaches, achieving the lowest MAE of 14 at  $q = 7$ , corresponding to a 3.1% error. These results underscore the advantage of CCL in ensuring collaboration only among highly correlated logical clusters.

CCL achieves the highest prediction accuracy by selectively collaborating with expert clusters; however, this improvement comes at a cost. Compared to FL, CCL incurs 5.5 times higher communication overhead, since models often converge to an optimal solution more quickly and are ready to collaborate, whereas FL requires a fixed number of epochs before aggregation. Moreover, FL suffers from higher MAE while offering only a 6.2% lower training time compared to CCL. Compared to GL, CCL reduces training time by 86.6%, demonstrating its efficiency. However, this improvement comes with 3.2 times higher memory usage than GL and 2.2 times more than FL, reflecting the computational cost of its collaborative approach. These results highlight CCL's ability to achieve the lowest MAE at the expense of increased communication and memory overhead. Detailed results are provided in the supplementary materials.

2) *DUPS*: Once CCL predicts the traffic and user count, these values are utilized by DUPS to pool DU servers. To demonstrate the versatility of DUPS across diverse traffic environments, three edges are selected based on their traffic characteristics. The first selected edge  $EC_{10}$  exhibits the highest traffic in the dataset, averaging 4.5 TBs, and comprises 108 BSs. The second edge,  $EC_3$ , represents a moderate-traffic environment with an average of 3.5 TBs and includes 89 BSs. The final edge,  $EC_{11}$ , represents a low-traffic scenario, averaging 1.89 TBs and consisting of 45 BSs. This selection enables the evaluation of DUPS in high, moderate, and low traffic scenarios, showcasing its adaptability across varying network conditions. Several experiments have been conducted to determine the optimal configuration parameters for the DRL environment in all three ECs, aimed at reducing the number of DU servers while maintaining fronthaul latency requirements. These parameters include  $\alpha$ ,  $\beta$  used in the reward function, and DU server capacity  $d$  and their selection, for all three selected edges are provided in the supplementary material.

DUPS is compared with conventional and state-of-the-art MILP strategies using the respective optimal values of  $\alpha$ ,  $\beta$ , and  $d$  for each of the three edges:  $EC_{10}$ ,  $EC_3$ ,  $EC_{11}$ . In the conventional approach, each BS keeps its DU server in an always-active state. Fig. 8 illustrates this comparison,

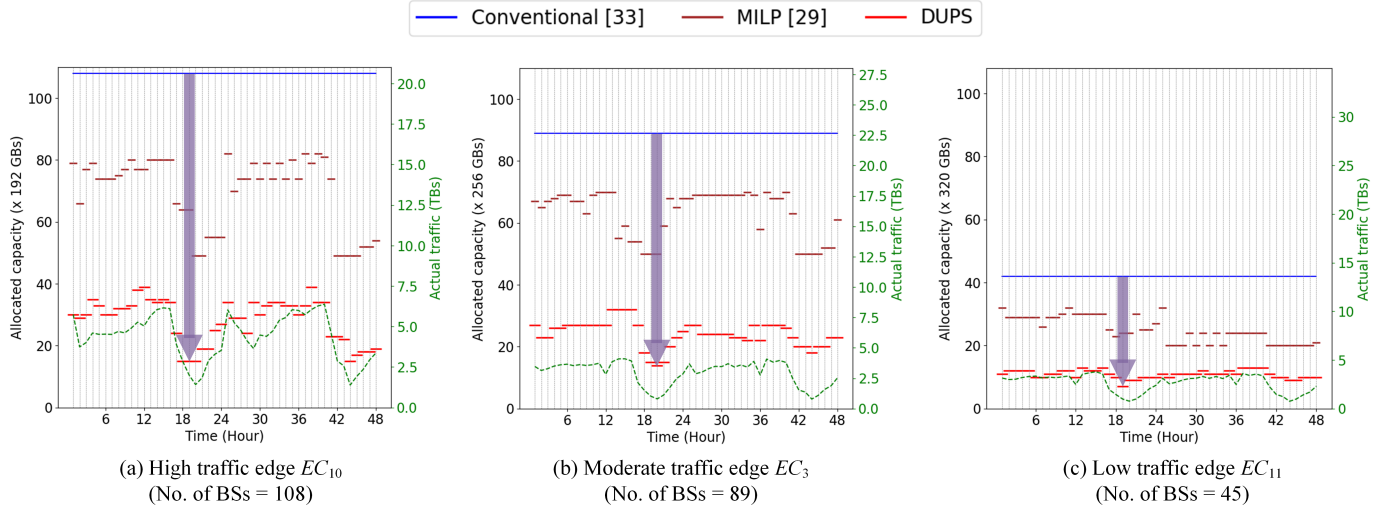


Fig. 8. Reduction in no. of DU servers by conventional, MILP, and DUPS in high, moderate, and low traffic edges.

TABLE I. Comparison of conventional [33], MILP [29], and DUPS in terms of average DU servers, power consumption, energy efficiency, and cost savings across high, moderate, and low traffic ECs. Power consumed per server is 650W [38] and cost per kWh  $r$  is USD 0.13 [39].

Edge traffic	Average DU servers			Power consumption reduction ( $p$ ) in Watts by DUPS compared to		Energy efficiency improvement (%) by DUPS compared to		Cost saved (USD/h) by DUPS compared to	
	Conv. $n_{conv.}$	MILP $n_{MILP}$	DUPS $n_{DUPS}$	Conv. $(n_{conv.} - n_{DUPS}) \times 650$	MILP $(n_{MILP} - n_{DUPS}) \times 650$	Conv. $\frac{n_{conv.} - n_{DUPS}}{n_{conv.}} \times 100$	MILP $\frac{n_{MILP} - n_{DUPS}}{n_{MILP}} \times 100$	Conv. $\frac{p \times r}{1000}$	MILP $\frac{p \times r}{1000}$
High	108	70	27	52650	44823	75	61.4	6844	5827
Moderate	89	63	24	42250	40276	74.1	57.1	5492	5235
Low	42	25	11	20150	15589	73.8	56.0	2619	2026

where the green dotted line represents the actual traffic of the respective ECs, the blue solid line shows the DU servers always active in the conventional approach [29], the brown line indicates the DU servers proposed by MILP [33], and the red line represents those managed by DUPS. For the high-traffic edge  $EC_{10}$ , DUPS achieves a significant reduction in the number of DU servers, particularly during low-traffic periods. During these periods, DUPS reduces the required DU servers by 89% and 81% compared to the conventional approach and MILP, respectively. This significant reduction is attributed to the efficient resource allocation by DUPS. For the moderate-traffic edge  $EC_3$ , DUPS reduces the number of DU servers by 86% and 77% compared to the conventional method and MILP approach, respectively. Finally, for the low-traffic edge  $EC_{11}$ , DUPS reduces the DU server count by 78% and 52% compared to the conventional approach and MILP, respectively. These reductions highlight the effectiveness of DUPS in resource management, delivering optimal performance and cost efficiency under varying network conditions.

Beyond its exceptional performance during low-traffic periods, DUPS is also evaluated for its effectiveness over the entire operational timeline. DUPS significantly improves energy efficiency and cost savings by reducing the number of active DU servers at any given time, as provided in Table I. A single DU server consumes approximately 650 Watts [38], equivalent to 0.65 kWh per hour. Thus, the total energy consumption for the conventional strategy is 0.65 times the number of active

DU servers. For the high-traffic edge  $EC_{10}$ , the conventional strategy requires 108 DU servers, which MILP reduces to an average of 70 servers, and DUPS further lowers to an average of 27 servers. In other words, DUPS achieves a 75% reduction in both the average number of servers and energy consumption compared to the conventional strategy and a 61.4% reduction compared to MILP. For the moderate-traffic edge, DUPS reduces the average number of servers and energy consumption by 74.1% compared to the conventional strategy and by 57.1% compared to MILP. Similarly, for the low-traffic edge, these reductions are 73.8% and 56%, respectively.

## V. CONCLUSION

This study addresses the high energy consumption in 5G RAN, which accounts for 50% of total power usage, highlighting the untapped potential of AI and deep learning to reduce OpEx while ensuring service quality. This paper presents DUPS, a solution that enhances energy efficiency by up to 89% and 75% compared to conventional methods and MILP, respectively, by turning off DU servers and redirecting their traffic. To achieve this, a DRL agent is assigned to each BS, making decisions to turn the server on or off. A single critic in the NWDAF calculates the reward and shares it back to each agent based on its contribution. This also includes a penalty if the DRL agent has forcefully turned off the DU server to save energy by violating latency requirements or due to insufficient capacity in the pool to which traffic is redirected.

Thus, a single policy is learned by the system based on the given traffic.

The substantial improvement offered by DUPS relies on accurate traffic prediction, achieved through the proposed CCL, which enhances prediction accuracy by enabling logical clusters to collaborate intelligently based on traffic correlation, sharing partial weights at optimal times. This enables logical clusters to effectively learn the missing information from one another. CCL employs MSTNet, which learns the spatio-temporal patterns from data. CCL is validated on a real cellular dataset from one of the biggest cities of Pakistan for traffic prediction, where it outperforms GL, FL, PFL, and CIIL methods by 43.9%, 39.1%, 40.8%, and 31.35%, respectively. A detailed evaluation shows that the proposed collaborative strategy delivers the best results in the tested settings, making DUPS with CCL essential for improving efficiency and optimizing network performance.

#### ACKNOWLEDGEMENTS

This work was partly supported by the Korea government (MSIT), IITP, Korea, under the ICT Creative Consilience program (IITP-2025-RS-2020-II201821, 30%); the Development of 6G Network Integrated Intelligence Plane Technologies (IITP-2025-RS-2024-00392332, 30%); and by the National Research Foundation of Korea (RS-2024-00343255, 40%).

#### DATA AND CODE AVAILABILITY

The complete dataset is private and cannot be publicly shared. However, a sample from one edge cloud is provided solely for research reference, along with the implementation code for all learning schemes and DUPS, at <https://github.com/Sardar-Jaffar-Ali/CCL-DUPS-EdgeAnalytics>.

#### REFERENCES

- [1] C. W. Zaw, N. H. Tran, Z. Han, and C. S. Hong, "Radio and computing resource allocation in co-located edge computing: A generalized nash equilibrium model," *IEEE Transactions on Mobile Computing*, vol. 22, no. 4, pp. 2340–2352, 2023.
- [2] 3GPP, "Study on new radio access technology: Radio access architecture and interfaces," 3GPP, Tech. Rep. 38.801, v14.0.0, 2017.
- [3] T. K. Rodrigues and N. Kato, "Hybrid centralized and distributed learning for mec-equipped satellite 6g networks," *IEEE Journal on Selected Areas in Communications*, vol. 41, no. 4, pp. 1201–1211, 2023.
- [4] K. V. Katsaros, E. Liotou, F. Moscatelli, T. Rokkas, G. Drainakis, E. Bonetto, D. Brevi, D. Klonidis, I. Neokosmidis, and A. Amditis, "Enabling far-edge intelligent services with network applications: The automotive case," *IEEE Internet of Things Magazine*, vol. 5, no. 4, pp. 122–128, 2022.
- [5] C. C. González, E. F. Pupo, E. Iradier, P. Angueira, M. Murrioni, and J. Montalbán, "Network selection over 5g-advanced heterogeneous networks based on federated learning and cooperative game theory," *IEEE Transactions on Vehicular Technology*, pp. 1–16, 2024.
- [6] J. Pei, S. Li, Z. Yu, L. Ho, W. Liu, and L. Wang, "Federated learning encounters 6g wireless communication in the scenario of internet of things," *IEEE Communications Standards Magazine*, vol. 7, no. 1, pp. 94–100, 2023.
- [7] M. Al-Quraan, L. Mohjazi, L. Bariah, A. Centeno, A. Zoha, K. Arshad, K. Assaleh, S. Muhaidat, M. Debbah, and M. A. Imran, "Edge-native intelligence for 6g communications driven by federated learning: A survey of trends and challenges," *IEEE Transactions on Emerging Topics in Computational Intelligence*, vol. 7, no. 3, pp. 957–979, 2023.
- [8] M. J. Sheller, B. Edwards, G. A. Reina, J. Martin, S. Pati, A. Kotrotsou, M. Milchenko, W. Xu, D. Marcus, R. R. Colen *et al.*, "Federated learning in medicine: facilitating multi-institutional collaborations without sharing patient data," *Scientific reports*, vol. 10, no. 1, 2020.
- [9] R. M. French, "Catastrophic forgetting in connectionist networks," *Trends in cognitive sciences*, vol. 3, no. 4, pp. 128–135, 1999.
- [10] S. J. Ali, S. M. Raza, and H. Choo, "Collaborative user mobility prediction in distributed edge computing framework," in *2024 IEEE 21st International Conference on Mobile Ad-Hoc and Smart Systems (MASS)*, 2024, pp. 288–294.
- [11] M. Chen, D. Gündüz, K. Huang, W. Saad, M. Bennis, A. V. Feljan, and H. V. Poor, "Distributed learning in wireless networks: Recent progress and future challenges," *IEEE Journal on Selected Areas in Communications*, vol. 39, no. 12, pp. 3579–3605, 2021.
- [12] B. McMahan, E. Moore, D. Ramage, S. Hampson, and B. A. y Arcas, "Communication-efficient learning of deep networks from decentralized data," in *Artificial intelligence and statistics*. PMLR, 2017, pp. 1273–1282.
- [13] L. Busoniu, R. Babuska, and B. De Schutter, "A comprehensive survey of multiagent reinforcement learning," *IEEE Transactions on Systems, Man, and Cybernetics, Part C (Applications and Reviews)*, vol. 38, no. 2, pp. 156–172, 2008.
- [14] V. Smith, C.-K. Chiang, M. Sanjabi, and A. S. Talwalkar, "Federated multi-task learning," in *Advances in Neural Information Processing Systems*, I. Guyon, U. V. Luxburg, S. Bengio, H. Wallach, R. Fergus, S. Vishwanathan, and R. Garnett, Eds., vol. 30. Curran Associates, Inc., 2017. [Online]. Available: [https://proceedings.neurips.cc/paper\\_files/paper/2017/file/6211080fa89981f66b1a0c9d55c61d0f-Paper.pdf](https://proceedings.neurips.cc/paper_files/paper/2017/file/6211080fa89981f66b1a0c9d55c61d0f-Paper.pdf)
- [15] Q. Wu, K. He, and X. Chen, "Personalized federated learning for intelligent iot applications: A cloud-edge based framework," *IEEE Open Journal of the Computer Society*, vol. 1, pp. 35–44, 2020.
- [16] M. J. Sheller, B. Edwards, G. A. Reina, J. Martin, S. Pati, A. Kotrotsou, M. Milchenko, W. Xu, D. Marcus, R. R. Colen *et al.*, "Federated learning in medicine: facilitating multi-institutional collaborations without sharing patient data," *Scientific reports*, vol. 10, no. 1, p. 12598, 2020.
- [17] M. A. Hossain, A. R. Hossain, W. Liu, N. Ansari, A. Kiani, and T. Saboorian, "A distributed collaborative learning approach in 5g+ core networks," *IEEE Network*, 2023.
- [18] H. Xia, X. Wei, Y. Gao, and H. Lv, "Traffic prediction based on ensemble machine learning strategies with bagging and lightgbm," in *2019 IEEE International Conference on Communications Workshops (ICC Workshops)*. IEEE, 2019, pp. 1–6.
- [19] I. Lohrasbina, A. Shahraki, A. Taherkordi, and A. Delia Jurcut, "From statistical to machine learning-based network traffic prediction," *Transactions on Emerging Telecommunications Technologies*, vol. 33, no. 4, p. e4394, 2022.
- [20] D. Alekseeva, N. Stepanov, A. Veprev, A. Sharapova, E. S. Lohan, and A. Ometov, "Comparison of machine learning techniques applied to traffic prediction of real wireless network," *IEEE Access*, vol. 9, pp. 159 495–159 514, 2021.
- [21] E. Tuna and A. Soysal, "Lstm and gru based traffic prediction using live network data," in *2021 29th Signal Processing and Communications Applications Conference (SIU)*. IEEE, 2021, pp. 1–4.
- [22] Z. Zhang, F. Li, X. Chu, Y. Fang, and J. Zhang, "dmt: A deep meta-learning based framework for mobile traffic prediction," *IEEE Wireless Communications*, vol. 28, no. 5, pp. 110–117, 2021.
- [23] Z. Liu, W. Li, J. Feng, and J. Zhang, "Research on satellite network traffic prediction based on improved gru neural network," *Sensors*, vol. 22, no. 22, p. 8678, 2022.
- [24] G. Chen, Y. Guo, Q. Zeng, and Y. Zhang, "A novel cellular network traffic prediction algorithm based on graph convolution neural networks and long short-term memory through extraction of spatial-temporal characteristics," *Processes*, vol. 11, no. 8, p. 2257, 2023.
- [25] S. P. Sone, J. J. Lehtomäki, and Z. Khan, "Wireless traffic usage forecasting using real enterprise network data: Analysis and methods," *IEEE Open Journal of the Communications Society*, vol. 1, pp. 777–797, 2020.
- [26] B. S. Shawel, E. Mare, T. T. Debell, S. Pollin, and D. H. Woldegebre, "A multivariate approach for spatiotemporal mobile data traffic prediction," *Engineering Proceedings*, vol. 18, no. 1, p. 10, 2022.
- [27] P. Wireless, "Open ran functional splits, explained," White paper, 2023.
- [28] L. M. M. Zorello, L. Blik, S. Troia, T. Guns, S. Verwer, and G. Maier, "Baseband-function placement with multi-task traffic prediction for 5g radio access networks," *IEEE Transactions on Network and Service Management*, vol. 19, no. 4, pp. 5104–5119, 2022.
- [29] M. Klinkowski, "Optimized planning of du/cu placement and flow routing in 5g packet xhaul networks," *IEEE Transactions on Network and Service Management*, vol. 21, no. 1, pp. 232–248, 2024.
- [30] C. C. Zhang, K. K. Nguyen, and M. Cheriet, "Joint routing and packet scheduling for urllc and ebb traffic in 5g o-ran," in *ICC 2022-IEEE*



- International Conference on Communications*. IEEE, 2022, pp. 1900–1905.
- [31] Y. Xiao, J. Zhang, Z. Gao, and Y. Ji, “Service-oriented du-cu placement using reinforcement learning in 5g/b5g converged wireless-optical networks,” in *2020 Optical Fiber Communications Conference and Exhibition (OFC)*. IEEE, 2020, pp. 1–3.
  - [32] Samsung, “Virtualized radio access network: Architecture, key technologies, and benefits,” Samsung, Technical Report, 2020. [Online]. Available: [https://images.samsung.com/is/content/samsung/assets/global/business/networks/insights/white-papers/virtualized-radio-access-network/white-paper\\_virtualized-radio-access-network\\_1.pdf](https://images.samsung.com/is/content/samsung/assets/global/business/networks/insights/white-papers/virtualized-radio-access-network/white-paper_virtualized-radio-access-network_1.pdf)
  - [33] Fujitsu, “Virtualized cu/du (vcu/du),” Blog, 2024. [Online]. Available: <https://www.fujitsu.com/global/products/network/products/vcuvdu/>
  - [34] Z. Wang, J. Fan, H. Wu, D. Sun, and J. Wu, “Representing multiview time-series graph structures for multivariate long-term time-series forecasting,” *IEEE Transactions on Artificial Intelligence*, vol. 5, no. 6, pp. 2651–2662, 2024.
  - [35] S. J. Ali, S. M. Raza, H. Yang, D. T. Le, R. Challa, M. Kim, and H. Choo, “In-time conditional handover for b5g/6g,” *Computer Communications*, p. 108107, 2025.
  - [36] H. Gupta, A. A. Franklin, M. Kumar, and B. R. Tamma, “Traffic-aware dynamic functional split for 5g cloud radio access networks,” in *2022 IEEE 8th International Conference on Network Softwarization (NetSoft)*. IEEE, 2022, pp. 297–301.
  - [37] 3GPP, “CU-DU split: Refinement for Annex A (Transport network and RAN internal functional split),” 3GPP, Tech. Rep. R3-162102, Oct 2016.
  - [38] Trenton Systems, “COTS Servers Product Brief,” 2024, accessed: 2024-06-07.
  - [39] C. Data, “Residential electricity price in south korea (usd per kwh),” 2021, accessed: January 2025. [Online]. Available: <https://www.ceicdata.com/en/korea/environmental-environmental-policy-taxes-and-transfers-oecd-member-annual/kr-residential-electricity-price-usd-per-kwh>